

**Quantitative dopant profiling in semiconductors: A Kelvin probe force microscopy model**

C. Baumgart, M. Helm, and H. Schmidt

*Institute of Ion Beam Physics and Materials Research, Forschungszentrum Dresden–Rossendorf e.V., P.O. Box 510119, 01314 Dresden, Germany*

(Received 14 July 2009; published 7 August 2009)

Kelvin probe force microscopy (KPFM) is used to investigate the electrostatic force between a conductive probe and nanostructured Si with shallow or buried selectively doped regions under ambient conditions. A unique KPFM model correlates the measured Kelvin bias with the calculated Fermi energy, and thus allows quantitative dopant profiling. We show that due to an asymmetric electric-dipole formation at the semiconductor surface the measured Kelvin bias is related with the difference between Fermi energy and respective band edge, and independent of the probe potential.

DOI: [10.1103/PhysRevB.80.085305](https://doi.org/10.1103/PhysRevB.80.085305)

PACS number(s): 61.72.uf, 07.79.–v

**I. INTRODUCTION**

Failure analysis and optimization of nanoelectronic devices demand knowledge of their electrical properties. For dopant profiling by means of scanning capacitance microscopy,<sup>1–3</sup> scanning spreading resistance microscopy,<sup>4–6</sup> or conducting atomic force microscopy<sup>7,8</sup> measurements, very sensitive capacitance, resistance, or conductivity sensors, respectively, have been developed. The corresponding sensor has to be attached onto the scanner head frame of the atomic force microscope (AFM). However, the above mentioned electrical nanometrology techniques only yield the quantitative dopant profile of semiconductors if they are used complementary and if calibration measurements have been performed on well-described reference samples. The most straightforward nanometrology technique is the Kelvin probe force microscopy (KPFM) where electrostatic forces are detected at a lock-in frequency below the resonance frequency of the conductive probe. KPFM is derived from a method developed by Lord Kelvin in 1898.<sup>9</sup> The Kelvin method was primarily combined with the AFM technique to investigate electrostatic forces between probe and metals,<sup>10</sup> and between probe and semiconductors.<sup>11</sup> After that KPFM has been used to investigate various aspects such as the interface dipole layer formed between a metal surface and alkali chloride thin films,<sup>12,13</sup> the tip-sample interaction,<sup>14,15</sup> dopant profiles in semiconductors<sup>16,17</sup> even with an atomic resolution,<sup>18</sup> *pn* junctions without<sup>19,20</sup> and under an applied bias,<sup>21,22</sup> or the electrostatic forces between probe and insulators, e.g., caused by the Madelung surface potential.<sup>23</sup> The Kelvin bias and topography can be probed simultaneously, as shown primarily by Lü *et al.* in 1999.<sup>24</sup> An interesting new field of nonquantitative applications of KPFM is the investigation of organic materials such as DNA and protein molecules on the nanometer scale.<sup>25,26</sup> In many biomolecules the local charge density around charge centers changes during the formation of binding complexes. By means of KPFM different binding complexes can be qualitatively distinguished. For example, Gao and Cai probed protein-DNA interactions.<sup>25</sup> The quantitative evaluation of KPFM data probed on biomolecules remains an open issue.

A broad field of applications of the KPFM technique is the quantitative dopant profiling in semiconductors. For

quantitative dopant profiling in semiconductors the measured Kelvin bias has to be evaluated with a correct physical model. Nonnenmacher *et al.*<sup>10</sup> interpreted the measured Kelvin bias as the contact potential difference (CPD) between a conductive probe and the sample material. Since then the CPD model, which is described in detail in the literature,<sup>10,27,28</sup> has been used to describe the Kelvin bias probed on semiconductors. Observed differences between the CPD simulation and KPFM measurement have been mainly ascribed to charges trapped in surface states.<sup>17,28–31</sup>

In this paper we introduce a unique KPFM model, and reveal a quantitative relation between the Kelvin bias and the difference between the calculated Fermi energy and respective band edge in selectively doped regions. We elucidate why the KPFM signal quantitatively depends on the bias necessary to inject majority charge carriers into the surface region. We tested our KPFM model successfully on two cross-sectionally prepared Si epilayer structures and on a Si dynamic random access memory (DRAM) cell with a native oxide layer, and correlated the measured Kelvin bias on *n*-type and *p*-type conducting regions with the calculated energy differences  $[E_C - E_F(n)]$  and  $[E_V - E_F(p)]$ , respectively. Traps in the oxide layer or defects at the oxide-semiconductor interface may cause the observed KPFM offset  $U_{off}$ .

**II. KELVIN PROBE FORCE MICROSCOPY ON SEMICONDUCTORS**

KPFM is a noncontact measurement technique where the electrostatic forces between a conductive probe and the sample surface are detected and minimized by applying an appropriate bias voltage. The basic measurement principle of the KPFM is schematically shown in Fig. 1. As given in Eq. (1) a dc voltage  $U_{dc}$  and an ac voltage  $U_{ac}$  are permanently applied to the sample while the probe is grounded during the KPFM measurement. In total the applied bias reads

$$U_{applied} = U_{dc} + U_{ac} \sin(2\pi f_{ac} t), \quad (1)$$

where  $U_{dc}$  is the sum of the KPFM offset bias  $U_{off}$  and the Kelvin bias  $U_K$ . The electrostatic forces between the conductive probe and the surface lead to a deflection of the probe from its normal position. For semiconductors the electro-

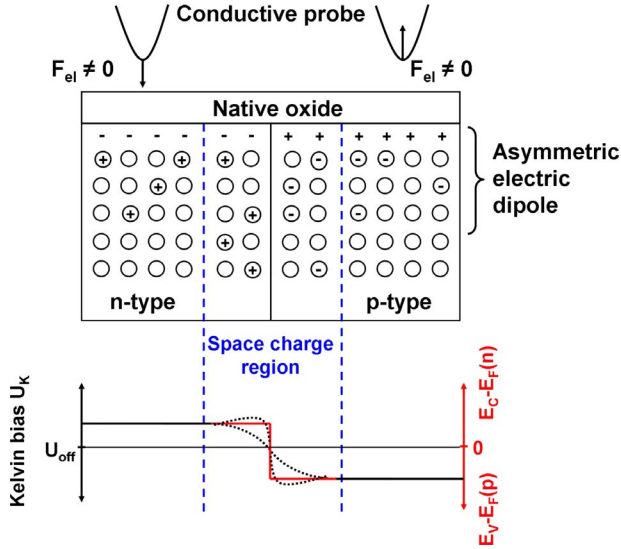


FIG. 1. (Color online) Surface-near region of a semiconductor with differently doped regions. An asymmetric electric dipole consisting of mobile charge carriers trapped in surface states (+, -) and the same number of unscreened immobile ionized dopant atoms is formed at the semiconductor surface, which causes a nonzero electrostatic force  $F_{el}$  at the position of the conductive probe. The electrostatic forces are minimized by injecting majority charge carriers into the surface region. The Kelvin bias may overshoot at the  $pn$  junction.

static forces onto the probe are caused by the electric-dipole formation at the semiconductor surface due to surface states. Surface states are occupied by electrons and holes in  $n$ -type and  $p$ -type semiconductors, respectively. As a consequence a depletion layer is formed without applying a bias to the sample. In a simple model we assume that the number of mobile charges being trapped in surface states is the same as the number of immobile unscreened ionized dopant atoms (Fig. 1). The electrostatic force  $F_{el}$  from this asymmetric electric dipole onto the conductive probe increases with the size asymmetry, and changes its direction above  $n$ -type and  $p$ -type regions. In order to minimize the electrostatic force  $F_{el}$  onto the probe, the asymmetric electric-dipole layer has to be removed. This is achieved by injecting majority charge carriers into the surface region in order to screen the unscreened immobile ionized dopant atoms. The charge neutrality condition is only fulfilled when surface states discharge simultaneously. Without the electrostatic force  $F_{el}$  (Fig. 1) the probe returns to its normal position. Accumulation of majority charge carriers is achieved by applying a dc voltage amounting to  $[E_C - E_F(n)]/e$  and  $[E_V - E_F(p)]/p$  in  $n$ -type and  $p$ -type regions, respectively. As a consequence, the measured Kelvin bias is correlated with the difference between Fermi energy and respective band edge, and *independent* of the probe potential. This relation is given in Eqs. (2) and (3), and illustrated in Fig. 2, where also the CPD is shown in comparison. From Eqs. (2) and (3) it follows that the KPFM signal decreases with increasing concentration of donor or acceptor ions. Furthermore, in the ideal case of no KPFM offset bias  $U_{off}$  the modeled KPFM signal  $U_K$  changes sign when probing  $p$ -type and  $n$ -type semiconducting regions,

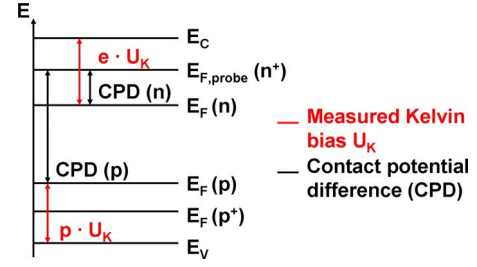


FIG. 2. (Color online) Schematic diagram of the measured Kelvin bias  $U_K$  by means of Kelvin probe force microscopy. Additionally, the CPD between a highly  $n^+$ -type probe and an  $n$ -type or  $p$ -type semiconductor is given. The CPD is not suitable to describe the measured Kelvin bias.

$$e \cdot U_K(n\text{-type}) = E_C - E_F(n), \quad (2)$$

$$p \cdot U_K(p\text{-type}) = E_V - E_F(p). \quad (3)$$

To date, the influence of surface states on KPFM measurements has not been clarified. We show that, using the data of Ref. 31 as an example, our KPFM model enables a quantitative data evaluation. Using the dopant profile from Ref. 31 our KPFM model predicts a difference of 320 mV between the KPFM data probed on the  $p^{++}$ -type and the  $n$ -type doped regions in a Si  $p^{++}n$  junction, which is in very good agreement with the measured Kelvin bias difference of approximately 300 mV. The reported overshoot of the measured Kelvin bias in the  $p^{++}$  region is possibly caused by the lateral electric field in the space-charge region, which will be explained later in detail. We conclude that surface states have to be included in order to explain the electrostatic force minimization by removing the asymmetric electric dipole, which forms between mobile charges trapped in surface states and unscreened immobile ionized dopant atoms. Furthermore, we expect that the KPFM offset bias  $U_{off}$  will be influenced by traps in the oxide layer or defects at the oxide-semiconductor interface.

As a direct consequence of the presented model a limitation of KPFM occurs when attempting to investigate  $p^{++}n^{++}$  junctions in semiconductors. With increasing concentration of ionized dopant atoms the differences  $[E_V - E_F(p)]/p$  and  $[E_C - E_F(n)]/e$  decrease until it is impossible to distinguish between  $p^{++}$  and  $n^{++}$  doped regions, where  $E_F$  has moved into the valence or the conduction band, respectively. Also the KPFM bias variation probed on metallic samples is very small.<sup>11</sup> On the other hand, reproducibly large KPFM variations up to 800 mV have been probed on metal-ionic samples<sup>12</sup> where dipoles at the interface between the metal and the ionic layers strongly influence the electrostatic force acting on the probe.

### III. CALCULATION OF THE FERMI ENERGY

The calculation of the Fermi energy needed for solving Eqs. (2) and (3) is based on the charge neutrality condition,<sup>32</sup>

$$p + N_D^+ = n + N_A^-. \quad (4)$$

In this equation  $n$  is the electron concentration in the conduction band and  $p$  is the hole concentration in the valence

band.  $N_D^+$  and  $N_A^-$  are the concentrations of ionized donors and acceptors, respectively. The energy position of the valence-band maximum  $E_V$  and the conduction-band minimum  $E_C$  does not have to be considered because only the differences  $[E_C - E_F(n)]$  and  $[E_V - E_F(p)]$  have to be calculated for a comparison with the measured Kelvin bias. The intrinsic Fermi energy of a semiconductor with  $N_D^+ = N_A^- = 0$  is defined as

$$E_F = E_i = \frac{E_V + E_C}{2} + \frac{k_B T}{2} \ln\left(\frac{N_V}{N_C}\right), \quad (5)$$

with  $k_B T = 0.0259$  eV at 300 K. We set  $E_i$  to zero on the energy scale. The Si valence- and conduction-band effective densities of states are  $N_V = 1.05 \times 10^{19}$  cm<sup>-3</sup> and  $N_C = 7.28 \times 10^{19}$  cm<sup>-3</sup>, respectively. The acceptor ionization energy  $E_A - E_V$  amounts to 0.045 eV for B acceptors and the donor ionization energy  $E_C - E_D$  amounts to 0.045 eV (0.054 eV) for P (As) donors.

#### IV. EXPERIMENTAL DETAILS

The KPFM measurements were performed under ambient conditions using an Anatec Level AFM. The Level AFM system consists of a base plate made from stone with wiring, vibration isolation, a standard AFM head, and a high-voltage amplifier V45C. The AFM head holds the cantilever by a spring-loaded mechanism. All electronic components for laser and photodiode, the lens and mirror system, and the fine mechanics are integrated in the head. The lateral resolution limit is smaller than 5 nm, practically achieved under ambient conditions. The height resolution is smaller than 0.2 nm, which enables the detection of atomic steps and layers. Both the resonance and the excited oscillation are evaluated with lock-in amplifiers, which are integrated fully digitally. The real part of the KPFM signal detected at the excited frequency, which is referred to as operation frequency, is used as the input signal for the digital Kelvin probe force feedback. This real part is maximized by using an autophase function. The Kelvin probe force feedback compensates the electrical force between probe and sample by applying the appropriate bias voltage. Topography and Kelvin bias are probed simultaneously. We used an operation frequency of 130 kHz. The resonance frequency of the cantilever was approximately 320 kHz. The effect of photogenerated charge carriers in the semiconducting sample was excluded by operating the whole Level AFM under an opaque cover.

Secondary ion mass spectrometry (SIMS) measurements were carried out to get information about the dopant concentration in differently doped areas of the epilayer structures. For detecting the positive or negative secondary ions formed from the species of interest, Cs<sup>+</sup> and O<sub>2</sub><sup>+</sup> ions were used for the primary beam. The analyzed raster size is given to be approximately 70 μm<sup>2</sup>. The chamber pressure during the SIMS measurement was approximately 2 × 10<sup>-9</sup> mbar. For KPFM measurements the Si epilayer samples were prepared cross sectionally. After cleaving, the sample pieces were embedded edgewise in synthetic resin, which is free of blow holes. Then, the back and front side of the resin barrels were lapped. The front side was additionally polished by using a

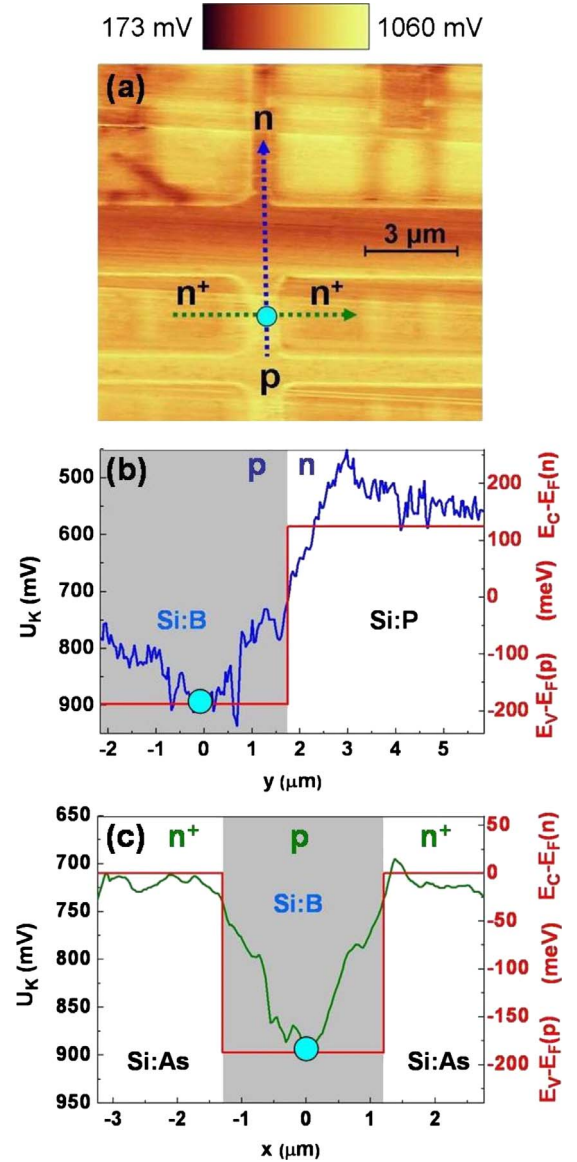


FIG. 3. (Color online) (a) Kelvin bias probed on a conventional Si dynamic random access memory cell. The size of the scan area is  $13 \times 13 \mu\text{m}^2$ . The top metal and dielectric layer were etched off to expose Si (Ref. 33). Calculated differences  $[E_C - E_F(n)]$  and  $[E_V - E_F(p)]$  in comparison to a  $U_K$  section line (b) across a  $pn$  junction and (c) across a  $n^+pn^+$  junction. The  $U_K$  section lines are averaged over 20 scan lines. The blue/light gray point lies on the origin of the coordinate system. The KPFM offset bias amounts to  $U_{\text{off}} = 710$  mV.

cloth with a grain size of 0.1 μm and an aluminum oxide cloth with a grain size of 0.04 μm. In the last preparation step a large Ohmic contact was deposited on the back side of the resin barrels.

#### V. RESULTS

Ultrashallow Si dopant profiles in a conventional DRAM cell<sup>33</sup> have been investigated. Figure 3(a) shows the measured Kelvin bias of the DRAM cell with the  $pn$  transition in

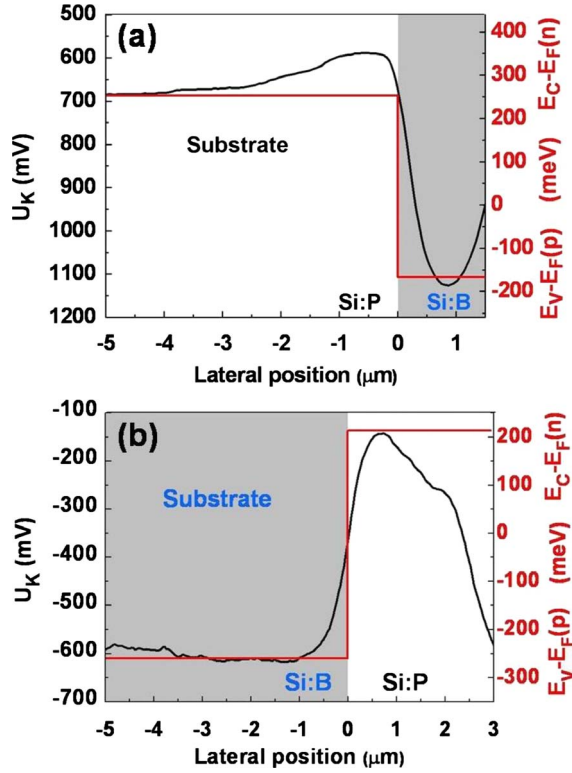


FIG. 4. (Color online)  $U_K$  section lines (averaged over 20 scan lines) of the Kelvin bias probed across  $pn$  junctions in cross-sectionally prepared Si epilayers in comparison to the calculated differences  $[E_C - E_F(n)]$  and  $[E_V - E_F(p)]$ ; (a) P-doped Si substrate with B-doped epilayers; (b) B-doped Si substrate with P-doped epilayers. The KPFM offset bias amounts to (a)  $U_{off}=950$  mV and (b)  $U_{off}=-350$  mV.

$y$  direction and the  $n^+pn^+$  transition in  $x$  direction. The  $pn$  section line crosses the  $p$ - and  $n$ -doped areas [Fig. 3(b)]. The  $n^+pn^+$  section line crosses the same  $p$ -doped area and highly  $n^+$ -doped areas [Fig. 3(c)]. For the  $pn$  junction in Fig. 3(b) with a B concentration of  $N_A=2 \times 10^{16} \text{ cm}^{-3}$  and a P concentration of  $N_D=2 \times 10^{17} \text{ cm}^{-3}$ , the CPD difference amounts to 810 meV. Our KPFM model predicts an energy difference of only 310 meV, which is in very good agreement with the measured Kelvin bias of approximately 300 mV. The  $n^+pn^+$  junction shown in Fig. 3(c) has an As concentration of  $N_D=2 \times 10^{20} \text{ cm}^{-3}$  and a B concentration of  $N_A=2 \times 10^{16} \text{ cm}^{-3}$ . Here the CPD difference amounts to 930 meV, whereas our KPFM model predicts a Kelvin bias difference of 190 mV being again in very good agreement with the measured Kelvin bias of approximately 200 mV. This key result strongly supports our KPFM model.

The interpretation of the Kelvin bias probed on a  $pn$  junction reveals another interesting aspect of the presented KPFM model, which is illustrated in Fig. 1. The lateral electric field in the space-charge region partially prevents the screening of the immobile ionized dopant atoms in the asymmetric electric-dipole layer at the semiconductor-oxide interface by injecting majority charge carriers into the surface region and will distort the probed Kelvin bias. The expected singularity of the Kelvin bias at the  $pn$  junction where the electric field has its maximum value may only be resolved

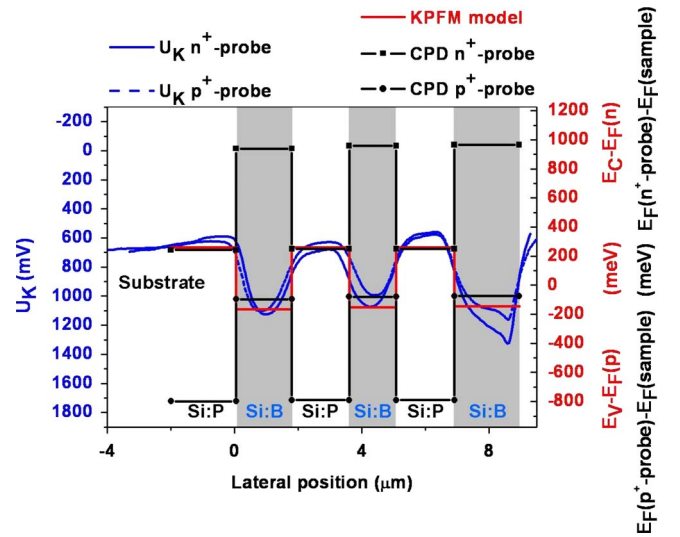


FIG. 5. (Color online)  $U_K$  section lines (averaged over 20 scan lines) of the Kelvin bias recorded across a cross-sectionally prepared Si epilayer structure compared to the calculated differences  $[E_C - E_F(n)]$  and  $[E_V - E_F(p)]$  with an  $n^+$ -type (solid blue/dark gray line) and a  $p^+$ -type (dashed blue/dark gray line) probe. The measured Kelvin bias  $U_K$  cannot be explained within the CPD model (black lines). The new KPFM model (red/gray line) reproduces the measured KPFM data independent of the probe potential. The KPFM offset bias amounts to  $U_{off}=950$  mV.

with an ultrasharp probe. Because at the end of the space-charge region the mobile charge density is smeared out over the Debye length; also there the probed Kelvin bias may be distorted.

Another dopant profile commonly met in Si is buried dopant profiles. We performed KPFM measurements on cross-sectionally prepared Si epilayer samples in order to probe such buried dopant profiles. In addition secondary-ion mass spectrometry was carried out to get information about the dopant profile in differently doped areas of the epilayer structures. In Fig. 4 the section lines of the Kelvin bias probed on different  $pn$  junctions of cross-sectionally prepared Si epilayer structures with a surface roughness less than 10 nm are represented. In Fig. 4(a) the Kelvin bias across a  $pn$  junction between two differently doped Si regions with a B concentration of  $N_A=4.7 \times 10^{16} \text{ cm}^{-3}$  and a P concentration of  $N_D=1.4 \times 10^{15} \text{ cm}^{-3}$  can be seen. The calculated CPD difference amounts to 700 meV, whereas our KPFM model predicts a Kelvin bias difference of 420 mV. This is in very good agreement with the measured Kelvin bias of approximately 440 mV. The Kelvin bias probed around the lateral position  $z=0 \mu\text{m}$  shows impressively the expected overshoot due to the lateral electric field in a  $pn$  junction (Fig. 1). In Fig. 4(b) the Kelvin bias probed on a  $pn$  junction between doped Si regions with a B concentration of  $N_A=1 \times 10^{15} \text{ cm}^{-3}$  and a P concentration of  $N_D=6.5 \times 10^{15} \text{ cm}^{-3}$  is shown. The CPD difference amounts to 650 meV, whereas our KPFM model predicts a Kelvin bias difference of 470 mV. Again this is in good agreement with the measured Kelvin bias difference of approximately 470 mV. The  $pn$  junction presented in Fig. 4(a) is a zoom in of the substrate-epilayer region in the cross-sectionally prepared

epilayer sample shown as a whole in Fig. 5. In addition to the  $n^+$ -probe NSC15/hd-P with a P concentration of  $N_D=5 \times 10^{19} \text{ cm}^{-3}$ , we also used the  $p^+$ -probe NSC15/hd-B, which has a B concentration of  $N_A=5 \times 10^{19} \text{ cm}^{-3}$ . According to the CPD model (Fig. 2) the Kelvin bias recorded with the  $p^+$ -type probe should differ by approximately 1000 mV from the Kelvin bias probed with the  $n^+$ -type probe in the substrate region (Fig. 5). However, the measured KPFM data are independent of the probe potential (Fig. 5). This can only be explained with our KPFM model.

## VI. CONCLUSIONS

In conclusion, a unique KPFM model for the interpretation of the Kelvin bias measured by means of KPFM has been presented and successfully tested on a conventional Si DRAM cell and on cross-sectionally prepared Si epilayer structures. The model allows correlating quantitatively of the measured Kelvin bias above  $n$ -type and  $p$ -type Si including  $pn$  junctions with the energy difference between the Fermi energy and the corresponding band edge. With the knowl-

edge about the concentration and the type of mobile charge carriers at a reference position, e.g., in the substrate region, or with the knowledge about the constant, offset of the KPFM signal, the KPFM model enables direct dopant profiling on the nanoscale in low to heavily doped semiconductors. We expect that for any material system a correct model of the asymmetric electric-dipole formation at the surface would allow relating of the measured Kelvin bias with the electrical properties of the investigated material system.

## ACKNOWLEDGMENTS

The authors would like to thank A.-D. Müller and F. Müller from Anfattec Instruments AG (Oelsnitz, Germany) for helpful discussions about the KPFM measurement technique. We also would like to thank A. Möller and P. Pelzing from SGS Institut Fresenius GmbH (Dresden, Germany) for their help with the sample preparation. Funding from Bundesministerium für Bildung und Forschung (BMBF) (Grant No. FKZ 03N8708) is gratefully acknowledged by H.S.

- <sup>1</sup>J. J. Kopanski, J. F. Marchiando, and J. R. Lowney, *Mater. Sci. Eng., B* **44**, 46 (1997).
- <sup>2</sup>F. Giannazzo, D. Goghero, V. Raineri, S. Mirabella, and F. Priolo, *Appl. Phys. Lett.* **83**, 2659 (2003).
- <sup>3</sup>F. Giannazzo, V. Raineri, S. Mirabella, E. Bruno, G. Impellizzeri, and F. Priolo, *Mater. Sci. Eng., B* **124-125**, 54 (2005).
- <sup>4</sup>L. Zhang, K. Ohuchi, K. Adachi, K. Ishimaru, M. Takayanagi, and A. Nishiyama, *Appl. Phys. Lett.* **90**, 192103 (2007).
- <sup>5</sup>L. Zhang, H. Tanimoto, K. Adachi, and A. Nishiyama, *IEEE Electron Device Lett.* **29**, 799 (2008).
- <sup>6</sup>P. De Wolf, W. Vandervorst, H. Smith, and N. Khalil, *J. Vac. Sci. Technol. B* **18**, 540 (2000).
- <sup>7</sup>K. Smaali, M. Troyon, A. El Hdiy, M. Molinari, G. Saint-Girons, and G. Patriarche, *Appl. Phys. Lett.* **89**, 112115 (2006).
- <sup>8</sup>M. Yamauchi, T. Inoshita, and Hiroyuki Sakaki, *Appl. Phys. Lett.* **74**, 1582 (1999).
- <sup>9</sup>L. Kelvin, *Philos. Mag.* **46**, 82 (1898).
- <sup>10</sup>M. Nonnenmacher, M. P. O'Boyle, and H. K. Wickramasinghe, *Appl. Phys. Lett.* **58**, 2921 (1991).
- <sup>11</sup>M. Nonnenmacher, M. P. O'Boyle, and H. K. Wickramasinghe, *Ultramicroscopy* **42-44**, 268 (1992).
- <sup>12</sup>C. Loppacher, U. Zerweck, and L. Eng, *Nanotechnology* **15**, S9 (2004).
- <sup>13</sup>U. Zerweck, C. Loppacher, T. Otto, S. Grafström, and L. M. Eng, *Phys. Rev. B* **71**, 125424 (2005).
- <sup>14</sup>H. O. Jacobs, P. Leuchtman, O. J. Homan, and A. Stemmer, *J. Appl. Phys.* **84**, 1168 (1998).
- <sup>15</sup>A. Liscio, V. Palermo, K. Müllen, and P. Samori, *J. Phys. Chem. C* **112**, 17368 (2008).
- <sup>16</sup>N. Duhayon, P. Eyben, M. Fouchier, T. Clarysse, W. Vandervorst, D. Alvarez, S. Schoemann, M. Ciappa, M. Stangoni, W. Fichtner, P. Formanek, M. Kittler, V. Raineri, F. Giannazzo, D. Goghero, Y. Rosenwaks, R. Shikler, S. Saraf, S. Sadewasser, N. Barreau, T. Glatzel, M. Verheijen, S. A. M. Mentink, M. von Sprekelsen, T. Maltezopoulos, R. Wiesendanger, and L. Hellmann, *J. Vac. Sci. Technol. B* **22**, 385 (2004).
- <sup>17</sup>A. K. Henning, T. Hochwitz, J. Slinkman, J. Never, S. Hoffmann, P. Kaszuba, and C. Daghljan, *J. Appl. Phys.* **77**, 1888 (1995).
- <sup>18</sup>M. Ligowski, D. Moraru, M. Anwar, T. Mizuno, R. Jablonski, and M. Tabe, *Appl. Phys. Lett.* **93**, 142101 (2008).
- <sup>19</sup>B.-Y. Tsui, C.-M. Hsieh, P.-C. Su, S.-D. Tzeng, and S. Gwo, *Jpn. J. Appl. Phys.* **47**, 4448 (2008).
- <sup>20</sup>M. Tanimoto and O. Vatel, *J. Vac. Sci. Technol. B* **14**, 1547 (1996).
- <sup>21</sup>A. Doukkali, S. Ledain, C. Guasch, and J. Bonnet, *Appl. Surf. Sci.* **235**, 507 (2004).
- <sup>22</sup>G. H. Buh, H. J. Chung, C. K. Kim, J. H. Yi, I. T. Yoon, and Y. Kuk, *Appl. Phys. Lett.* **77**, 106 (2000).
- <sup>23</sup>F. Bocquet, L. Nony, C. Loppacher, and T. Glatzel, *Phys. Rev. B* **78**, 035410 (2008).
- <sup>24</sup>J. Lü, E. Delamarche, L. Eng, R. Bennewitz, E. Meyer, and H.-J. Güntherodt, *Langmuir* **15**, 8184 (1999).
- <sup>25</sup>P. Gao and Y. Cai, *Anal. Bioanal. Chem.* **394**, 207 (2009).
- <sup>26</sup>A. K. Sinensky and A. M. Belcher, *Nat. Nanotechnol.* **2**, 653 (2007).
- <sup>27</sup>T. Mizutani, T. Usunami, S. Kishimoto, and K. Maezawa, *Jpn. J. Appl. Phys., Part 2* **38**, L767 (1999).
- <sup>28</sup>A. Kikukawa, S. Hosaka, and R. Imura, *Appl. Phys. Lett.* **66**, 3510 (1995).
- <sup>29</sup>S. Sadewasser, Th. Glatzel, R. Shikler, Y. Rosenwaks, and M. Ch. Lux-Steiner, *Appl. Surf. Sci.* **210**, 32 (2003).
- <sup>30</sup>Y. Rosenwaks, R. Shikler, Th. Glatzel, and S. Sadewasser, *Phys. Rev. B* **70**, 085320 (2004).
- <sup>31</sup>S. Saraf, M. Molotskii, and Y. Rosenwaks, *Appl. Phys. Lett.* **86**, 172104 (2005).
- <sup>32</sup>S. M. Sze, *Physics of Semiconductor Devices*, 2nd ed. (John Wiley and Sons, New York, 1981).
- <sup>33</sup>Application note AN079, Electrical characterization with Scanning capacitance probe microscopes, Veeco Instruments (2008).